PCCP

PAPER

Cite this: *Phys. Chem. Chem. Phys.*, 2019, **21**, 14005

Isotope-selective chemistry in the $Be^+(^2S_{1/2})$ + HOD → $BeOD^+/BeOH^+$ + H/D reaction

Gary K. Chen,[a] Changjian Xie,[b] Tiangang Yang, *[a] Anyang Li, [c] Arthur G. Suits, [d] Eric R. Hudson,[a] Wesley C. Campbell[a] and Hua Guo *[b]

Received 28th October 2018,
Accepted 20th December 2018

DOI: 10.1039/c8cp06690f

rsc.li/pccp

Low temperature reactions between laser-cooled $Be^+(^2S_{1/2})$ ions and partially deuterated water (HOD) molecules have been investigated using an ion trap and interpreted with zero-point corrected quasi-classical trajectory calculations on a highly accurate global potential energy surface for the ground electronic state. Both product channels have been observed for the first time, and the branching to $BeOD^+$ + H is found to be 0.58 ± 0.14. The experimental observation is reproduced by both quasi-classical trajectory and statistical calculations. Theoretical analyses reveal that the branching to the two product channels is largely due to the availability of open states in each channel.

1. Introduction

Together, isotope substitution and the measurement of the resulting product branching ratios provide important details about reaction dynamics and are often used to identify reaction pathways and understand bond-selective chemistry.[1–3] Important examples include X + HOD (X = H, F, Cl, O) reactions, where the branching ratios are experimentally controlled by selective excitation of the O–H or O–D bond.[4–12] It is now understood that a highly-accurate potential energy surface (PES) is crucial for performing theoretical calculations of the product branching ratio, where subtle, difficult to identify, PES features have been found to significantly affect the results.[13]

A sophisticated understanding of radical-molecule reaction dynamics is continuing to develop from extensive experimental and theoretical studies. However, despite their importance in interstellar chemistry, where the isotopic branching ratios strongly influence the products of the interstellar cloud chemical network,[14] far less progress has been made in the study of ion–molecule reactions at low temperature. This is largely due to the challenges associated with both the experimental and theoretical approaches to these systems.[15–21] Experimental difficulties include a lack of quantum state preparation and readout techniques, while theoretical difficulties appear when treating dynamics dominated by the long range interaction between ions and molecules. Recently, several groups have employed cold (~mK) and fully-controlled laser-cooled trapped ions to address these experimental issues. For instance, isotope selectivity was probed in the reaction of laser-cooled Mg^+ with HD,[22] and the formation rate of MgD^+ was found to be 5 times greater than MgH^+. This observation was ascribed to a dynamic mechanism in the exit channel of the reaction since statistical methods predict only a factor of approximately 2.[23] A similar experimental technique was applied to Ca^+ + HD reactions as well,[24] where the CaD^+ channel was found to have ~1.5 times higher population than the CaH^+ channel; no detailed theoretical calculations have been performed for this system. With the help of laser-cooled ions, the initial quantum states are experimentally well controlled, but highly accurate PESs are still challenging to calculate with Mg^+ or Ca^+ ions due to the complexity of their electronic structures. The development of a more comprehensive understanding of ion–molecule reactions at low temperature will benefit from studies with less complex species that are amenable to theoretical treatment.

In this publication, we report a combined experimental and theoretical study of the effect of isotope substitution in an ion–polyatomic molecule reaction. A key objective is to understand the role of dynamics in such a reaction. Previous work on $Be^+ + H_2O$ showed that chemical dynamics resulting from a submerged barrier strongly affect the reaction, leading to a reduction of the overall reaction rate from the capture limit. The overestimation by the capture model was thus taken as a sign that this reaction is not completely statistical, despite the existence of a deep BeH_2O^+ potential well along the reaction path. In this work, we probe the dynamics by examining the product branching ratio, which is presumably controlled by the exit channel barriers. Such a measurement is much more

[a] *Department of Physics and Astronomy, University of California Los Angeles, Los Angeles, California 90095, USA. E-mail: yangtiangang@g.ucla.edu*
[b] *Department of Chemistry and Chemical Biology, University of New Mexico, Albuquerque, New Mexico 87131, USA. E-mail: hguo@unm.edu*
[c] *Key Laboratory of Synthetic and Natural Functional Molecule Chemistry, Ministry of Education, College of Chemistry and Materials Science, Northwest University, 710127 Xi'an, P. R. China*
[d] *Department of Chemistry, University of Missouri, Columbia, Missouri 65211, USA*

sensitive to the determination of the overall rates. Interestingly, here we find that the measured deuteration fraction of the ionic products is in good agreement with quasi-classical trajectory (QCT) calculations on the ground state PES. Furthermore, the branching ratio can be explained by a statistical model based on complete energy randomization in the long-lived transition complex.

2. Experimental

The apparatus employed here has been described in detail elsewhere.[25] Briefly, laser ablation of metallic Be is used to produce Be^+ ions, which are trapped in a linear radio frequency Paul trap. Laser cooling[26] is used to cool the translational motion of the ions, resulting in a Coulomb crystal of Be^+ ions. A time-of-flight mass spectrometer (TOF-MS)[27–30] is integrated into the Paul trap to analyze reaction products, allowing investigation of the isotope effect by mass spectrometry of the trapped ionic products. The 313 nm laser for cooling Be^+ ions allows manipulation of the Be^+ electronic quantum states; by tuning the frequency of this cooling laser, the fraction of ions in the $^2S_{1/2}$ and $^2P_{3/2}$ states can be precisely controlled. Promotion of the Be^+ to the $^2P_{3/2}$ state opens more product pathways, as well as modifies existing product channels.[25]

HOD is made by mixing H_2O and D_2O.[31,32] The gaseous room-temperature $HOD/H_2O/D_2O$ mixture is then introduced *via* a leak valve into the trapping region for reaction with the trapped ions, the actual ratio of the mixture is measured from a Stanford Research Systems (SRS) residual gas analyzer (RGA). The RGA's fractionation of water was calibrated by introducing the water vapor into the chamber and integrating all resulting m/z signals. A typical scan reveals water fractionation products at m/z = 18, 17, and 16, which coincide with H_2O^+, OH^+, and O^+. The fractionation ratios of water are found by solving the system of equations:

$$P_{H_2O} = R_{18} + R_{17} + R_{16} \quad (2.1)$$

$$R_{18} = \alpha P_{H_2O} \quad (2.2)$$

$$R_{17} = \beta P_{H_2O} \quad (2.3)$$

$$R_{16} = \gamma P_{H_2O} \quad (2.4)$$

where R_i is the pressure reading from the RGA and P_{H_2O} is the true H_2O pressure. These fragmentation ratios were found to be $\alpha = 0.768 \pm 0.006$, $\beta = 0.184 \pm 0.006$ and $\gamma = 0.068 \pm 0.002$. The direct readings from analog scans with deuterated samples were then adjusted to account for the fractionation for each isotopologue.

$$P_{H_2O} = \frac{1}{\alpha}\left(R_{18} + \frac{\beta}{\alpha}R_{20} + \frac{\beta}{2\alpha}R_{19}\right) \quad (2.5)$$

$$P_{H_2O} = \frac{R_{19}}{\alpha} \quad (2.6)$$

$$P_{D_2O} = \frac{R_{20}}{\alpha} \quad (2.7)$$

where P_i are the real adjusted partial pressures for each isotopologue.

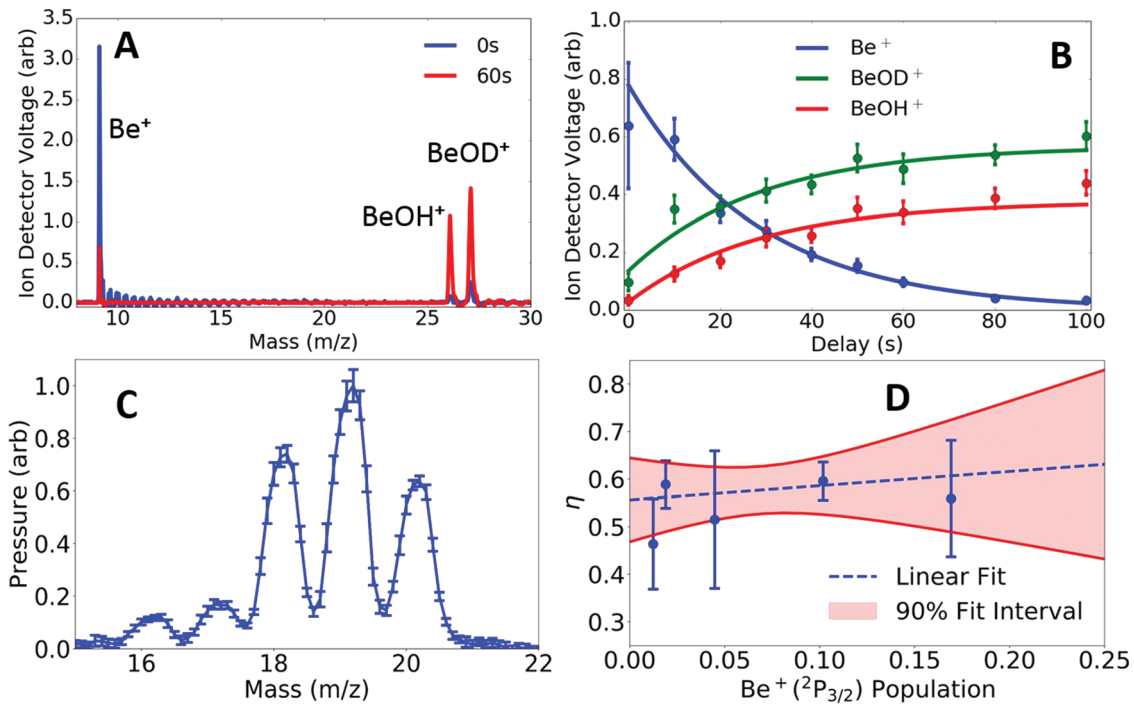

Fig. 1 (A) A typical TOF signal (5 sample average) at reaction time t = 0 s and 60 s with $P_P \approx 2\%$. (B) The temporal evolution of Be^+, $BeOH^+$ and $BeOD^+$ in the trap as a function of reaction time as well as the solutions of differential equations fitted to the kinetics data with $P_P \approx 2\%$. (C) The RGA signal (8 traces average) gives relative initial H_2O, HOD, D_2O sample ratio, which is $\rho_1 : \rho_2 : \rho_3 = (1.00 \pm 0.02) : (2.45 \pm 0.05) : (1.58 \pm 0.02)$. (D) The product fraction for $BeOD^+$ production (η) of reaction (4.2) as a function of $Be^+(^2P_{3/2})$ state population. The S-state branching ratio is found to be $\eta_s = 0.56 \pm 0.03$, in agreement with the following calculated combined value with different initial H fractions.

Ionic products of the chemical reaction remain in the trap, and are subsequently detected *via* TOF-MS. Product branching ratios are extracted from the mass spectrum. A typical TOF spectrum (5 sample average) at reaction time t = 0 and 60 s with 2% relative Be^+ $^2P_{3/2}$ state excitation and a full reaction curve are shown in Fig. 1A and B, respectively. Since the translational energy of the laser-cooled Be^+ ions is less than 0.5 K, the energy of the room temperature water sets the reaction kinetic energy of $Be^+ + H_2O/D_2O/HOD$ in the center of mass frame to $\bar{E}_{col}/k_B \approx$ 100 K. The initial internal state distribution of the molecules is assumed to be at 300 K. To maintain consistent collision temperatures as well as mass spectra resolution, while predominantly probing S-state reactions, weak laser cooling is used, which promotes ≈2% of Be ions into the P-state.

3. Theoretical

Quasi-classical trajectory calculations

The QCT calculations were performed with VENUS[33] to study the reaction dynamics of the $Be^+ + D_2O/HOD$ reaction. The $Be^+ + H_2O$ reaction has been studied in our previous work using the same method. The global PES for ground electronic state of this system was from our previous work.[25] Although the ground state has a conical intersection with the first excited state in the product channel,[25] the excellent agreement between theory and experiment suggests the adiabatic approximation is valid. In this work, we use the single-state adiabatic approximation in our dynamic calculations. The reaction path, including the energies of the stationary points for the Be^+ + HOD reaction, is shown in Fig. 2.

The trajectories were initiated with a 41.0 Å separation between reactants, and terminated when products reached a separation of 8.0 Å. The atomic coordinates and momenta of the reactant D_2O/HOD were sampled randomly using a Monte Carlo approach, based on a Boltzmann distribution at 300 K with the zero-point energy (ZPE) of the molecule defined as the energy zero. The collision energy is sampled from a Boltzmann distribution of 100 K. The largest impact parameter was chosen to be b_{max} = 39 Å for proper inclusion of long-range interactions. The propagation time step was chosen as 0.05 fs. The conservation of total energy was found to be better than 0.020 kcal mol^{-1} for all the trajectories. The possible violation of the ZPE for both the reactant and product molecules was corrected using the approach proposed by Paul and Hase.[34] Only those trajectories with the vibrational energies of $HOD/D_2O/BeOD^+/BeOH^+$ larger than the corresponding ZPEs are accepted. Those with vibrational energies below the respective ZPE are turned back to the interaction region by changing the sign of the atomistic momenta. A trajectory is discarded if its propagation time reached 300 ps in each interval of two consecutive momentum reversing operations, or when the number of momentum reversing events exceeds 100. Only a few such trajectories were found.

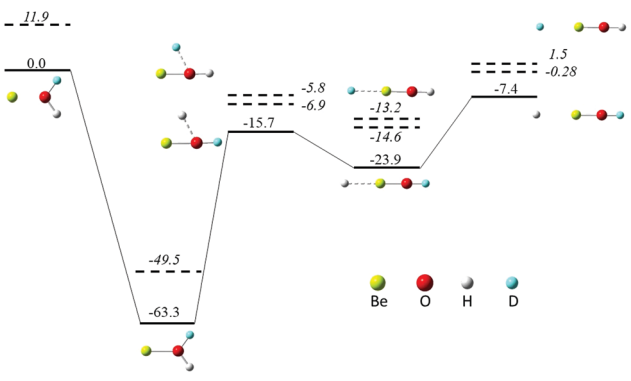

Fig. 2 Schematic energetics (in kcal mol^{-1}) for the $Be^+ + HOD \rightarrow BeOH^+ + D/BeOD^+ + H$ reaction path on its ground electronic state. The energetics and geometry of the stationary points are also given. Dashed lines include the ZPEs (italic numbers) for indicated species.

The thermal rate constant can be computed by:

$$k(T) = \left(\frac{8k_BT}{\pi\mu}\right)^{1/2} \pi b_{max}^2 \frac{N_r}{N_t}, \quad (3.1)$$

where N_r and N_t are the numbers of reactive and total trajectories, respectively. μ is the reduced mass between reactants Be^+ and D_2O/HOD, k_B is the Boltzmann constant, b_{max} is the maximum impact parameter, and T is the translational temperature in Kelvin. In our calculations, a total of 2×10^4 trajectories were run for each of the $Be^+ + D_2O$ and $Be^+ + HOD$ reactions.

The scattering angle θ is defined here as

$$\theta = \cos^{-1}\left(\frac{\vec{v}_i \cdot \vec{v}_f}{|\vec{v}_i||\vec{v}_f|}\right), \quad (3.2)$$

where $\bar{v}_i$ is the relative velocity vector of the reactants $\bar{v}_{Be}$–$\bar{v}_{H_2O}$ and $\bar{v}_f$ is the relative vector $\bar{v}_{BeOH}$–$\bar{v}_H$ corresponding to the products. (For deuterated reactants and products, the vectors are defined analogously.) The reactive differential cross section (DCS) can be then calculated by

$$\frac{d\sigma_r}{d\Omega} = \frac{\sigma_r P_r(\theta)}{2\pi \sin\theta}, \quad (3.3)$$

where $P_r(\theta)$ is the probability for the scattering of the products at the angle θ, and σ_r is integral cross section (ICS)

$$\sigma_r = \pi b_{max}^2 \frac{N_r}{N_t}. \quad (3.4)$$

Statistical model

We adapt the phase-space theory (PST) of Light and Pechukas in determining the branching ratio of products $BeOD^+/BeOH^+$ as a function of the collision energy.[35,36] For the Be^+ + HOD reaction, the conservation of total energy requires

$$E_T = E_c^i + E(v_i^1, v_i^2, v_i^3, j_i) = E_c^f + E(v_f^1, v_f^2, v_f'^2, v_f^3, j_f), \quad (3.5)$$

where the symbols v and j denote collectively the vibrational and rotational quantum numbers of the reactant HOD and products $BeOH^+/BeOD^+$, i and f refer to the initial and final states, and 1, 2, 3 represent the three vibrational modes of the reactant and products. For the linear products $BeOH^+/BeOD^+$,

there are four vibrational quantum numbers because the bending vibration is doubly degenerate. E is the internal energy, E_c is the collision energy. In the calculations, the reactant HOD was assumed to be in various ro-vibrational states populated at 300 K.

For a given initial collision energy E_c^i in the reactant channel, the total energy E_T can be determined. Thus, the total number (N) of the energetically available products $BeOH^+/BeOD^+$ ro-vibrational states can be computed by

$$N(E_T) = \sum_{|j_f - l_f| \le J \le |j_f + l_f|} \sum_{l_f} \sum_{v_f^1, v_f^2, v_f'^2, v_f^3, j_f} n\left(v_f^1, v_f^2, v_f'^2, v_f^3, j_f, l_f, J; E_T\right), \tag{3.6}$$

in which l_f and J are the orbital and total rotational quantum numbers of the reaction system, and J ranges from $|j_f - l_f|$ to $|j_f + l_f|$. The value of $n(v_f^1, v_f^1, v_f'^2, v_f^3, j_f, l_f, J; E_T)$ is 0 or 1 depending on whether the channel is open or not. Specifically, it equals 1 when the internal energy of the product state $E(v_f^1, v_f^2, v_f'^2, j_f)$ satisfies the following two conditions:

(1) It is below the total energy E_T;

(2) The corresponding collision energy E_c^f is larger than the centrifugal barrier with l_f in the minimum energy path (V_{MEP}) of product D + $BeOH^+$/H + $BeOD^+$. The centrifugal barrier was determined with respect to the asymptote of the product channel by

$$V_{cent}(R) = \frac{l(l+1)}{2\mu_R R^2} + V_{MEP}(R), \tag{3.7}$$

where R is the distance between atom D/H and center of mass of $BeOH^+/BeOD^+$, μ_R is the reduced mass. Otherwise, $n(v_f^1, v_f^2, v_f'^2, v_f^3, j_f, l_f, J; E_T)$ is zero. The parity ($(-1)^{J+j_f+l_f}$) was also constrained by the quanta ($v_f^2 + v_f'^2$) of bending mode of the linear products $BeOH^+$ and $BeOD^+$. Even/odd quanta of $v_f^2 + v_f'^2$ can only be available in even/odd parities. For the product molecules, the internal energy is computed using the harmonic oscillator and rigid rotor approximations. Finally, the product channel fractions at the translational temperature of 100 K are obtained by integrating the energy dependent branching ratio with a Boltzmann weight. To converge the results, the initial collision energy is chosen from 0 to 0.91 kcal mol^{-1} to account for Boltzmann weights larger 0.01. For the highest collision energy, the maximum of l is 69 and 90 for the H + $BeOD^+$ and D + $BeOH^+$ channels, respectively.

To simulate the 300 K internal temperature in the reactant, the HOD ro-vibrational energies are computed using the harmonic oscillator and rigid rotor approximations. For the asymmetric top reactant HOD, the rigid rotor Hamiltonian matrix for a given total rotational quantum momentum J is ($\hbar = 1$),[37]

$$\begin{aligned} H_{K',K''} &= \frac{1}{2}[(2C - A - B)K'^2 + (A + B)J(J+1)]\delta_{K'K''} \\ &+ \frac{1}{4}(B - A)\sqrt{J(J+1) - K'(K'+1)}\sqrt{J(J+1) - (K'+1)(K'+2)}\delta_{K'+2K''} \\ &+ \frac{1}{4}(B - A)\sqrt{J(J+1) - K'(K'-1)}\sqrt{J(J+1) - (K'-1)(K'-2)}\delta_{K'-2K''} \end{aligned} \tag{3.8}$$

where K is the projection of the J on the I_a axis, A, B, and C are the rotational constants of HOD calculated at its equilibrium structure (A = 23.05 cm^{-1}, B = 9.11 cm^{-1}, C = 6.53 cm^{-1}). The rotational energy levels then can be obtained by diagonalizing the above Hamiltonian matrix. The ZPEs for the reactant HOD and products $BeOH^+$ and $BeOD^+$ are 11.69, 8.94, and 7.16 kcal mol^{-1}, respectively. At 300 K, the Boltzmann averaged ro-vibrational energy of reactant HOD is 12.28 kcal mol^{-1}, which is 0.59 kcal mol^{-1} higher than its ZPE.

4. Results and discussion

Because the HOD sample also contains both H_2O and D_2O, the product $BeOH^+$ (m/z = 26) has contributions of the reaction of the cation with H_2O, while $BeOD^+$ (m/z = 27) has contributions from reactions with D_2O. The reactions of interest are:

$$Be^+(^2S_{1/2}) + H_2O \rightarrow BeOH^+ + H \tag{4.1}$$

$$\begin{aligned} Be^+(^2S_{1/2}) + HOD &\rightarrow BeOD^+ + H \\ &\rightarrow BeOH^+ + D \end{aligned} \tag{4.2}$$

$$Be^+(^2S_{1/2}) + D_2O \rightarrow BeOD^+ + D \tag{4.3}$$

Thus, the kinetics of the reagents and products are found from:

$$Be^+(t)' = -(k_1\rho_1 + k_2\rho_2 + k_3\rho_3)Be^+(t) \tag{4.4}$$

$$BeOH^+(t)' = (k_1\rho_1 + (1 - \eta)k_2\rho_2)Be^+(t) \tag{4.5}$$

$$BeOD^+(t)' = (k_3\rho_3 + \eta k_2\rho_2)Be^+(t) \tag{4.6}$$

where k_i and ρ_i are the rate coefficient and density for Be^+ reacting H_2O, HOD, and D_2O respectively. The branching ratio $\eta = k_{BeOD^+}/(k_{BeOD^+} + k_{BeOH^+})$ is the fraction of $BeOD^+$ produced from reactions (4.2) where k_j is the rate coefficient of species j.

Solutions to the rate equations (4.4)–(4.6) are parameterized by the density measurements of the water isotopologues taken from a RGA, and a least-squares fit is taken over data sets of integrated TOF mass spectra with shared fitting parameters k_1, k_2, k_3, and η.

In order to extract the pure $Be^+(^2S_{1/2})$ and $Be^+(^2P_{3/2})$-state branching ratios, the process shown in Fig. 1(A)–(C) was repeated at different P-state fractions. The results are shown in Fig. 1(D) along with a least-squares linear-fit (blue line). The vertical intercept of this fit gives $\eta_s = 0.56 \pm 0.03$ for the ground

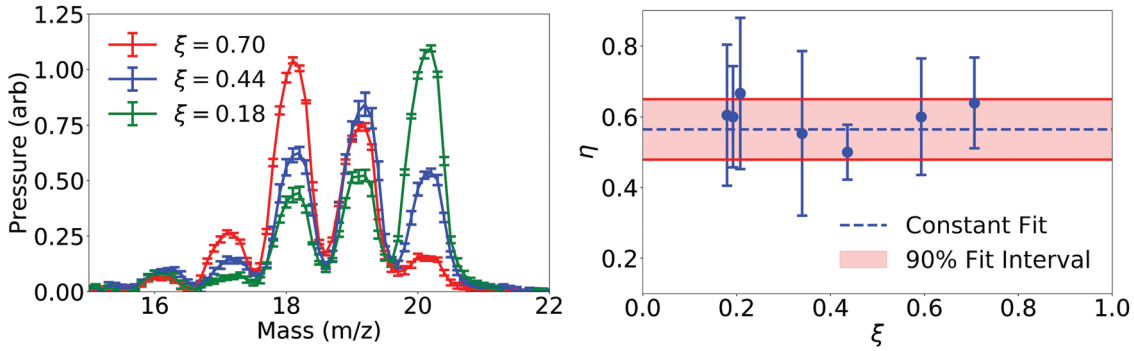

Fig. 3 (left) Averaged (8 traces) RGA analog scan showing peaks at each isotopologue m/z. Points around the peak of each isotopologue were averaged for a more accurate partial pressure. (right) The branching ratio η of the reaction Be^+ + HOD into $BeOD^+$ + H (with a Be^+ P-state fraction of ~2%) as a function of initial H fraction in an HOD, H_2O, D_2O mixture. Shared fitting the branching ratio η with a constant value fit is shown with a weighted average of $\eta = 0.58 \pm 0.14$.

$Be^+(^2S_{1/2})$ state reaction, while no conclusive dependence on P-state fractions is found within the confidence intervals.

To further verify that our measurement is independent of reagent ratios, we repeated the measurement for different mixtures of HOD, H_2O, and D_2O, as shown in Fig. 3. The branching ratio of $BeOD^+$ + H in reaction Be^+ + HOD (with 2% $Be^+(^2P_{3/2})$ state population) is consistent over different hydrogen fractions in the gas. The fraction of hydrogen atoms in the chamber (ξ) from all water isotopologues is defined by:

$$\xi = \frac{2\rho_{H_2O} + \rho_{HOD}}{2\rho_{H_2O} + 2\rho_{HOD} + 2\rho_{D_2O}}. \quad (4.7)$$

Weighted averaging of the fitted values over different mixtures then gives $\eta = 0.58 \pm 0.14$, $\frac{k_2}{k_1} = 0.8 \pm 0.9$, $\frac{k_3}{k_1} = 0.8 \pm 0.9$. Despite the large error bars on the relative rate coefficients, due to the significant covariance of the rate coefficients, η is reasonably well determined. To further check our measurement of η, the process was repeated for shared fits with identical rate coefficients ($k_1 = k_2 = k_3$) yielding $\eta = 0.57 \pm 0.07$.

The calculated overall rate coefficients of the Be^+ + D_2O and Be^+ + HOD reactions are $(2.29 \pm 0.05) \times 10^{-9}$ cm^3 molecule^{-1} s^{-1} and $(2.29 \pm 0.05) \times 10^{-9}$ cm^3 molecule^{-1} s^{-1}, respectively, which are slightly larger than that ($(2.02 \pm 0.04) \times 10^{-9}$ cm^3 molecule^{-1} s^{-1})[25] of the Be^+ + H_2O reaction. The calculated k_2/k_1 and k_3/k_1 ratios are 1.13 ± 0.04 and 1.13 ± 0.04, which are consistent with experimental values of 0.8 ± 0.9 and 0.8 ± 0.9, respectively. The identical k_2/k_1 and k_3/k_1 ratios suggests the negligible isotopic effect in the thermal reaction probabilities of the Be^+ + D_2O and Be^+ + HOD reactions.

The branching ratio was determined using the QCT method for the Be^+ + HOD reaction. Specifically, the calculated branching fraction of Be^+ + HOD (η) is 0.61 ± 0.02, which is in good agreement with experimental value 0.58 ± 0.14.

The branching ratio of the two products ($BeOD^+$ and $BeOH^+$) can be understood in terms of the PST model, which assumes complete energy randomization in the deep intermediate ($BeHOD^+$) well. In Fig. 4, the branching fraction for the $BeOD^+$ + H channel is plotted as a function of the collision energy,

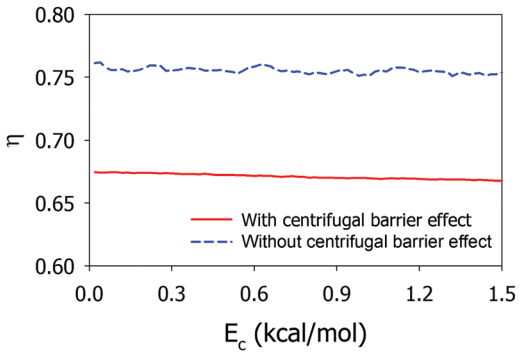

Fig. 4 PST branching fraction (η) of the $BeOD^+$ + H product channel as a function of the initial collision energy.

which shows very weak temperature dependence. At the specific collisional temperature 100 K, the fraction obtained by integrating the energy dependent branching ratio with a Boltzmann weight is 0.67, which is in reasonable agreement with the QCT results.

To shed more light onto the preference of the H + $BeOD^+$ channel in the Be^+ + HOD reaction, we provide a further analysis of the two important factors in determining the branching ratio. In PST, the reactivity in a particular product channel is controlled by the availability of open states, which is in turn dictated by the rovibrational states of the corresponding product molecule above the exit barrier formed by the centrifugal potential. Due to the heavier deuterium, it is readily understood that there are more rovibrational states for $BeOD^+$ than $BeOH^+$. However, the availability of open channels is also constrained by the orbital angular momentum (l), which erects a centrifugal barrier in both the reactant and product channels. The l-dependent centrifugal barrier is also isotope dependent, due to the difference in the reduced mass between the two products. The centrifugal barrier rises faster in the $BeOD^+$ + H channel than the $BeOH^+$ + D channel, due to the larger reduced mass of the latter. This is consistent with the fact that the branching fraction (η) of $BeOD^+$ + H channel becomes larger when the centrifugal barrier was not considered (shown in Fig. 4).

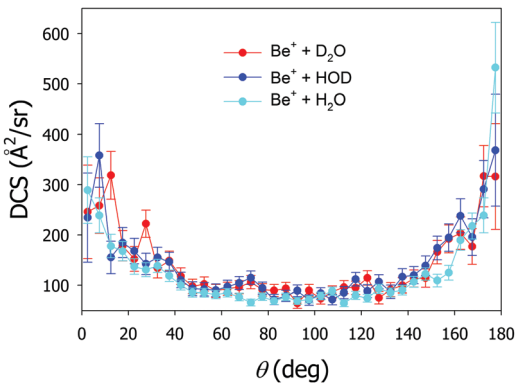

Fig. 5 Total DCSs of the $Be^+ + H_2O/HOD/D_2O$ reactions. Error bars denote the statistical errors in QCT calculations.

These two factors have opposing effects on the branching ratio, but the higher density of states in the $BeOD^+$ molecule dominates, at least at low energies. As a result, the $H + BeOD^+$ product channel is strongly favored. The good agreement of the statistical model with both the experimental and QCT results in branching ratio suggests that the reaction is largely statistical.

In addition, the DCSs of the $Be^+ + H_2O/HOD/D_2O$ reactions calculated by the QCT method are shown in Fig. 5. It can be seen from the figure that the DCSs of all three reactions are roughly forward–backward symmetric, due to the long-lived intermediates formed in the reactions. The forward–backward symmetry in DCSs suggests the statistical nature of the reaction, which further validates the suitability of the PST model discussed above.

5. Conclusions

To summarize, chemical reactions between $Be^+(^2S_{1/2})$ and HOD have been investigated using an integrated ion trap and high-resolution TOF-MS and ZPE corrected QCT calculations on an accurate global PES. Two product channels have been observed and the branching to $BeOD^+ + H$ is accurately determined to be 0.58 ± 0.14. The experimental result is in good agreement with ZPE corrected QCT calculation result (0.61 ± 0.02) as well as close to the statistical PST model (~ 0.67), which reveals that the branching to the two product channels is largely due to the availability of different open states in each channel. Since their rate coefficients deviate from the capture limit as reported in our earlier work, it is clear that the $Be^+(^2S_{1/2}) + H_2O/D_2O/HOD$ reactions have a non-negligible non-statistical component. Interestingly, however, the good prediction of the branching ratio by the statistical model discussed above suggests that the formation of the products is largely statistical. This conclusion is further supported by the forward–backward symmetry of the calculated DCSs.

Conflicts of interest

There are no conflicts to declare.

Acknowledgements

This work was funded by the Air Force Office of Scientific Research grant no. FA9550-16-1-0018. The UNM team is supported by the Air Force Office of Scientific Research (Grant No. FA9550-15-1-0305 to H. G.). A. L. acknowledges the support of the Key Science and Technology Innovation Team of Shanxi Province (2017KCT-37).

References

1 F. F. Crim, *Science*, 1990, **249**, 1387–1392.
2 F. F. Crim, *J. Phys. Chem.*, 1996, **100**, 12725–12734.
3 R. N. Zare, *Science*, 1998, **279**, 1875–1879.
4 A. Sinha, M. C. Hsiao and F. F. Crim, *J. Chem. Phys.*, 1990, **92**, 6333–6335.
5 M. J. Bronikowski, W. R. Simpson, B. Girard and R. N. Zare, *J. Chem. Phys.*, 1991, **95**, 8647–8648.
6 R. B. Metz, J. D. Thoemke, J. M. Pfeiffer and F. F. Crim, *J. Chem. Phys.*, 1993, **99**, 1744–1751.
7 D. H. Zhang and J. C. Light, *J. Chem. Soc., Faraday Trans.*, 1997, **93**, 691–697.
8 H. Song and H. Guo, *J. Chem. Phys.*, 2015, **142**, 174309.
9 J. Li, H. Song and H. Guo, *Phys. Chem. Chem. Phys.*, 2015, **17**, 4259–4267.
10 H. Song, S.-Y. Lee, Y. Lu and H. Guo, *J. Phys. Chem. A*, 2015, **119**, 12224–12230.
11 B. Fu and D. H. Zhang, *J. Chem. Phys.*, 2015, **142**, 064314.
12 R. Zheng, Y. Zhu and H. Song, *J. Chem. Phys.*, 2018, **149**, 054304.
13 D. Skouteris, D. E. Manolopoulos, W. Bian, H.-J. Werner, L.-H. Lai and K. Liu, *Science*, 1999, **286**, 1713–1716.
14 T. J. Millar, *Space Sci. Rev.*, 2003, **106**, 73–86.
15 D. C. Clary, *Annu. Rev. Phys. Chem.*, 1990, **41**, 61–90.
16 C. E. Dateo and D. C. Clary, *J. Chem. Soc., Faraday Trans.*, 1989, **85**, 1685–1696.
17 N. G. Adams and D. Smith, *Int. J. Mass Spectrom. Ion Phys.*, 1976, **21**, 349–359.
18 P. B. Armentrout, *Annu. Rev. Phys. Chem.*, 2001, **52**, 423–461.
19 I. R. Sims and I. W. M. Smith, *Annu. Rev. Phys. Chem.*, 1995, **46**, 109–138.
20 I. W. M. Smith and B. R. Rowe, *Acc. Chem. Res.*, 2000, **33**, 261–268.
21 T. P. Snow and V. M. Bierbaum, *Annu. Rev. Anal. Chem.*, 2008, **1**, 229–259.
22 P. F. Staanum, K. Højbjerre, R. Wester and M. Drewsen, *Phys. Rev. Lett.*, 2008, **100**, 243003.
23 N. F. Dalleska, K. C. Crellin and P. B. Armentrout, *J. Phys. Chem.*, 1993, **97**, 3123–3128.
24 A. K. Hansen, M. A. Sørensen, P. F. Staanum and M. Drewsen, *Angew. Chem., Int. Ed.*, 2012, **51**, 7960–7962.
25 T. Yang, A. Li, G. K. Chen, C. Xie, A. G. Suits, W. C. Campbell, H. Guo and E. R. Hudson, *J. Phys. Chem. Lett.*, 2018, **9**, 3555–3560.
26 D. J. Wineland and W. M. Itano, *Phys. Rev. A: At., Mol., Opt. Phys.*, 1979, **20**, 1521–1540.

27 S. J. Schowalter, K. Chen, W. G. Rellergert, S. T. Sullivan and E. R. Hudson, *Rev. Sci. Instrum.*, 2012, **83**, 043103.
28 C. Schneider, S. J. Schowalter, K. Chen, S. T. Sullivan and E. R. Hudson, *Phys. Rev. Appl.*, 2014, **2**, 034013.
29 P. Puri, M. Mills, C. Schneider, I. Simbotin, J. A. Montgomery, R. Côté, A. G. Suits and E. R. Hudson, *Science*, 2017, **357**, 1370–1375.
30 W. Paul, *Rev. Mod. Phys.*, 1990, **62**, 531–540.
31 J. W. Pyper, R. S. Newbury and G. W. Barton Jr., *J. Chem. Phys.*, 1967, **46**, 2253–2257.
32 S. A. Harich, X. Yang, X. Yang and R. N. Dixon, *Phys. Rev. Lett.*, 2001, **87**, 253201.
33 X. Hu, W. L. Hase and T. Pirraglia, *J. Comput. Chem.*, 1991, **12**, 1014–1024.
34 A. K. Paul and W. L. Hase, *J. Phys. Chem. A*, 2016, **120**, 372–378.
35 J. C. Light, *J. Chem. Phys.*, 1964, **40**, 3221–3229.
36 P. Pechukas and J. C. Light, *J. Chem. Phys.*, 1965, **42**, 3281–3291.
37 I. N. Levine, *Molecular spectroscopy*, Wiley, 1975.